THE JOURNAL OF BIOLOGICAL CHEMISTRY
Vol. 273, No. 50, Issue of December 11, pp. 33803–33810, 1998

Printed in U.S.A.

Changes in Microtubule Protofilament Number Induced by Taxol Binding to an Easily Accessible Site

INTERNAL MICROTUBULE DYNAMICS*

(Received for publication, September 9, 1998, and in revised form, September 29, 1998)

J. Fernando Díaz‡§, José M. Valpuesta¶, Pablo Chacón‡, Greg Diakun‖, and José M. Andreu‡**

From the ‡Centro de Investigaciones Biológicas, CSIC, Velázquez 144, 28006, Madrid, Spain, the §Laboratorium voor Chemische en Biologische Dynamica, Katholieke Universiteit Leuven, Celestijnenlaan 200D, B-3001 Leuven, Belgium, the ¶Centro Nacional de Biotecnología, CSIC-UAM, Cantoblanco, 28049 Madrid, Spain, and the ‖Daresbury Laboratory, CCLRC, Warrington WA4 4AD, United Kingdom

We have investigated the accessibility of the Taxol-binding site and the effects of Taxol binding on the structures of assembled microtubules. Taxol and docetaxel readily bind to and dissociate from microtubules, reaching 95% ligand exchange equilibrium in less than 3 min under our solution conditions (microtubules were previously assembled from GTP-tubulin, GTP-tubulin and microtubule-associated proteins, or GDP-tubulin and taxoid). Microtubules assembled from purified tubulin with Taxol are known to have typically one protofilament less than with the analogue docetaxel and control microtubules. Surprisingly, Taxol binding and exchange induce changes in the structure of preformed microtubules in a relatively short time scale. Cryoelectron microscopy shows changes toward the protofilament number distribution characteristic of Taxol or docetaxel, with a half-time of ~0.5 min, employing GDP-tubulin-taxoid microtubules. Correspondingly, synchrotron x-ray solution scattering shows a reduction in the mean microtubule diameter upon Taxol binding to microtubules assembled from GTP-tubulin in glycerol-containing buffer, with a structural relaxation half-time of ~1 min. These results imply that microtubules can exchange protofilaments upon Taxol binding, due to internal dynamics along the microtubule wall. The simplest interpretation of the relatively fast taxoid exchange observed and labeling of cellular microtubules with fluorescent taxoids, is that the Taxol-binding site is at the outer microtubule surface. On the contrary, if Taxol binds at the microtubule lumen in agreement with the electron crystallographic structure of tubulin dimers, our results suggest that the inside of microtubules is easily accessible from the outer solution. Large pores or moving lattice defects in microtubules might facilitate the binding of taxoids, as well as of possible endogenous cellular ligands of the inner microtubule wall.

Microtubules are dynamic polar polymers of $\alpha\beta$-tubulin dimers. A Mg^{2+} ion coordinated with non-exchangeable GTP bound to the α-subunit near the α-β dimerization interface controls the stability of the heterodimer (1), whereas the cation and exchangeable nucleotide bound to the β-subunit, near the β-α axial interface leading to protofilament formation (2) control microtubule stability. GTP hydrolysis in the polymers and GDP/GTP exchange in dimers originate phases of microtubule growth and shrinkage from the ends (dynamic instability). Most microtubules are closed pseudohelical cylinders. There are seams in the microtubule lattices in which the lateral intersubunit contacts are different from the rest of the wall (reviewed in Ref. 3). Microtubule end-growth *in vitro* proceeds by elongation of protofilament sheets which later close into a cylindrical wall (4). Among other cellular processes, microtubules are essential for the assembly of the mitotic spindle during cell division (5). Taxol[1] is an anticancer drug which arrests cell division by binding to and stabilizing microtubules (6–9). Taxol promotes *in vitro* microtubule assembly (10) and makes microtubules last longer. For these reasons it is extensively used experimentally, including studies of motor proteins and MAPs interacting with the microtubule surface (11–17).

Taxol can drive otherwise inactive GDP-tubulin into microtubule assembly. Binding of exactly one taxoid molecule per tubulin dimer and microtubule elongation are thermodynamically linked processes (18, 19). On the other hand, binding of Taxol to a few percent of the tubulin molecules in microtubules assembled from GTP-tubulin kinetically suppresses microtubule dynamic instability (20, 21).

Microtubules are typically formed by 13 protofilaments (22). However, this is a relatively flexible property of tubulin assembly. Transitions in the number of protofilaments have been observed along individual *in vitro* assembled microtubules (23). The number of protofilaments is fixed *in vivo* to 13 or other numbers by microtubule organizing centers and tubulin isoforms (24–26). The majority of microtubules assembled from purified tubulin with Taxol have 12 protofilaments, that is, one protofilament less than control microtubules, as shown by x-ray solution scattering, thin sectioning, and cryoelectron microscopy (27). However, microtubules induced by the side chain analogue docetaxel (Taxotere) have on average 13.4 protofilaments, similarly to control microtubules (28). Interestingly, during Taxol- and docetaxel-induced microtubule assembly, bidimensional polymers consisting of open protofilament

* This work was supported in part by Direccion General de Ensenante Superior Grant PB95-0116, the European Union Large Installations Program, Katholieke Universiteit Leuven Grant OT/93/20, and Nationale Funds voor Wetenschappelijk Onderzoek-Vlaanderen Grant 2.0163.94. The costs of publication of this article were defrayed in part by the payment of page charges. This article must therefore be hereby marked "*advertisement*" in accordance with 18 U.S.C. Section 1734 solely to indicate this fact.

** To whom correspondence should be addressed. Fax: 34-91-5627518; E-mail: j.m.andreu@fresno.csic.es.

[1] The abbreviations used are: Taxol® (paclitaxel), 4,10-acetoxy2α-(benzoyloxy)-5β,20-epoxy-1,7β-dihydroxy-9-oxotax-11-en-13α-yl-(2*R*, 3*S*)3[(phenylcarbonyl)amino]-2-hydroxy-3-phenylpropionate; MAPs, microtubule associated proteins; docetaxel (Taxotere®), 4-acetoxy-2α-(benzoyloxy)-5β,20-epoxy-1,7β,10β-trihydroxy-9-oxotax-11-en-13α-yl-(2*R*,3*S*)-3-[(*tert*-butoxycarbonyl)amino]-2-hydroxy-3-phenylpropionate; Mes, 4-morpholine- ethanesulfonic acid; GMP-PCP, guanosine β,γ-methyl- enediphosphonate.

sheets, which later close into microtubules, have been detected with time-resolved x-ray solution scattering (29).

The axial center to center spacing between tubulin monomers along one protofilament is typically 4.06 nm for the GDP-tubulin inside microtubules (30). However, with the γ-phosphate of the slowly hydrolyzable GTP analogue GMP-PCP, this spacing is 4.20 nm (31). The spacing with GDP relates to the "curved" inactive conformation of GDP-tubulin at depolymerizing microtubule ends, which spontaneously self-associates forming double rings (made of curved protofilament segments), whereas the expanded conformation with GMP-PCP relates to the "straight" active conformation of GTP-tubulin which can assemble into microtubules (32–37). Interestingly, in Taxol-induced microtubules the tubulin monomers are in the expanded conformation (38–39).

Taxol also induces modifications in the rheologic properties of microtubules, consisting of changes in flexural rigidity (40–45) and a reported spiral curling (41). In addition, Taxol makes microtubules less susceptible to orientation in high magnetic fields (46).

One obvious question is what happens when taxoids bind to steady state assembled microtubules (47, 48). Will the assembled structures remain with the same protofilaments until they disassemble and assemble again? Will the protofilament number and the axial spacing slowly relax to the Taxol values? Arnal and Wade (39) have indicated that Taxol addition modifies only slightly the structure of assembled microtubules in comparison to assembly with Taxol, however, they did not report quantification of the Taxol binding in their study. On the other hand, during our studies of taxoid-induced assembly (27–29) we acquired preliminary synchrotron x-ray solution scattering data indicating that Taxol addition to preassembled microtubules decreases their diameter. We reasoned that Taxol binding to microtubules should ultimately lead to the same final equilibrium state as direct assembly with Taxol, the only problem being the kinetics of the process. That is, depending on the solution conditions, the polymers might in practice remain locked in the non-Taxol state for a longer time than the experimental observation (or than the average lifetime of microtubules), or their structures will relax toward the Taxol state. Here we report measurements of taxoid binding to assembled microtubules, Taxol and docetaxel ligand exchange in the polymer-binding site, and measurements of microtubule structural changes with cryoelectron microscopy and x-ray scattering. The results show that taxoids readily bind to and dissociate from microtubules, and give compelling evidence that Taxol changes the protofilament number of microtubules made of purified tubulin in a subminute time scale. These novel results and the location of Taxol in the electron crystallography model structure of tubulin (49) indicate previously unexpected features of microtubule structure and function.

EXPERIMENTAL PROCEDURES

Tubulin, Taxoids, and Microtubules—Purified calf brain tubulin, GDP-tubulin preparation, and chemicals were as described (18). GDP-tubulin was equilibrated in PEDTA buffer (10 mM sodium phosphate, 1 mM EDTA, 1 mM GDP) to which 7 or 8 mM $MgCl_2$ was added, final pH 6.7. For comparative purposes, GTP-tubulin was obtained by addition of 1 mM GTP to GDP-tubulin aliquots with $MgCl_2$. For glycerol-induced assembly, tubulin was directly equilibrated in glycerol assembly buffer, 10 mM sodium phosphate, 3.4 M glycerol, 1 mM EGTA, 1 mM GTP, to which 6 mM $MgCl_2$ was added, final pH 6.7. All tubulin samples were clarified by centrifugation at 50,000 rpm, 4 °C, during 10 min in TL100.2 and TL100.3 rotors in Beckman TL100 centrifuges before $MgCl_2$ addition. Microtubule protein, containing tubulin and MAPs, was prepared as described (50) in 100 mM Mes, 1 mM EGTA, 1 mM $MgSO_4$, 1 mM GTP, pH 6.7. Taxol was kindly provided by the late Dr. M. Suffness, National Cancer Institute, NIH (Bethesda, MD). [^{3}H]Taxol was a gift from Drs. I. Ringel, The Hebrew University (Jerusalem) and S. B. Horwitz, Albert Einstein College of Medicine (Bronx, NY). Docetaxel (Taxotere) and [^{14}C]docetaxel were kindly provided by Rhône-Poulenc Rorer (92165 Antony, France).

Binding of Taxoids to Microtubules: Competition and Dissociation Measurements—Microtubules were assembled for 1 h at 37 °C in glycerol assembly buffer, then different amounts of taxoid or the corresponding volume of Me_2SO (typically <1%, v/v) were added, and the samples incubated for 30 min at 37 °C. The amounts of bound and free taxoid were measured using a radioactive method as described (18).

To measure equilibrium competition between taxoids for binding to microtubules, GDP-tubulin was assembled at 37 °C in PEDTA buffer containing 1 mM GDP and 8 mM $MgCl_2$, by the addition of Taxol or docetaxel. One hour after the competitor ligand was added and the bound and free taxoids were quantified after an additional 1 h. In control measurements microtubules were directly assembled with the mixture of both Taxol and docetaxel.

The time course of the displacement of taxoids was measured as follows. GDP-tubulin was assembled with taxoid as above and diluted to a concentration at which the displacement could be effectively measured, *i.e.* 5 μM for Taxol assembled samples, and 3 μM for the docetaxel assembled samples, a 6-fold excess of the displacing ligand was added and samples were taken at different times of reaction, and bound Taxol and docetaxel were quantified as above.

Electron Microscopy Determination of Microtubule Protofilament Number—The time course of the change of the number of protofilaments with taxoids was examined as follows. GDP-tubulin (10 μM) in PEDTA buffer containing 1 mM GDP and 8 mM $MgCl_2$ was assembled by adding an equimolecular concentration of taxoid, the sample was left to assemble for 1 h and then diluted and excess competitor taxoid added exactly as in the taxoid displacement experiments above. Samples were taken at different times of reaction and were processed for electron microscopy. Alternatively, GTP-tubulin (>50 μM) was assembled in glycerol assembly buffer for 30 min at 37 °C. Taxol, docetaxel, at an equimolecular concentration with tubulin, or Me_2SO were added samples were taken at different times of reaction and were processed by electron microscopy. Electron micrographs of negatively stained samples were recorded as described (28).

Samples for cryoelectron microscopy were incubated at 37 °C at various times of taxoid exchange and aliquots were transferred to holey grids that had been previously glow discharged. The grids were blotted and plunged into liquid ethane. Electron micrographs were obtained using a JEOL JEM 1200EX II operated at 120 kV and recorded on Kodak SO-163 film. Images were taken at a magnification of ×30,000 with a 20–25 μm underfocus. A GATAN-626 cold stage was used in the recording of the micrographs from the specimens.

Lateral views of microtubules contain characteristic longitudinal fringe patterns which are generated by the projection of the protofilaments in the front and back of the microtubule wall. This is due to tilting of the microtubule lattice with respect to the microtubule axis, resulting in a protofilament twist, in order to accommodate more or less than the characteristic 13 protofilaments of a nearly paraxial lattice. Lattice tilting is required to achieve correct cylindrical closure of the tubulin monomers within the lattice, as exemplified with microtubule models and geometrical calculations (27, 51). The number of protofilaments corresponding to each image in this work were classified from the type of fringe pattern (27, 51). This method has been widely employed (28, 39, 52, 53). In addition, the orientation of the moiré fringe patterns in cryoelectron micrographs allows determination of microtubule polarity (54).

X-ray Scattering by Microtubule Solutions—Measurements were made at station 2.1 of the Daresbury Laboratory Synchrotron Radiation Source, UK. Data acquisition and processing, interpretation of the microtubule x-ray scattering, and computer modeling were as described previously (27–29, 55). A scanning temperature-controlled cell was employed throughout the measurements, which made radiation damage negligible. Cameras (2 and 3 m) and a 512-channel quadrant ionization detector were employed, effectively covering a S range from 0.02 to 0.35 nm^{-1}. S is the absolute value of the scattering vector, defined as $S = 2(\sin\theta)/\lambda$, where 2θ is the angle of the scattered to incident radiation and λ the x-ray wavelength. To monitor the time course of the J_{01} and J_{02} scattering maxima, the scattering profiles were acquired in 1-s time frames after isothermal mixing, employing a fast mixing device with a 0.1-s dead time (56). The scattering intensity was corrected for radial dilution multiplying by the scattering vector. To reduce noise to an acceptable level the scattering profiles were averaged in 10-s intervals. The J_{01} and J_{02} peaks were fitted by third order polynomials, and the discrete S value (channel) closest to the maximum taken as the position of the J_0 peak. The changes in position of the

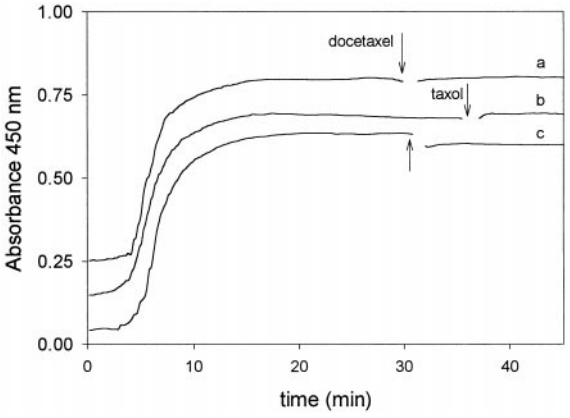

FIG. 1. **Effect of taxoid addition on assembled microtubules.** The time course of assembly of 70 μM GTP-tubulin in glycerol assembly buffer 37 °C was monitored turbidimetrically. At the steady state positions marked by the *arrows*, 80 μM docetaxel (*a*), Taxol (*b*) or the volume of Me_2SO in which these drugs were dissolved (*c*), were added (final Me_2SO <1%, v/v).

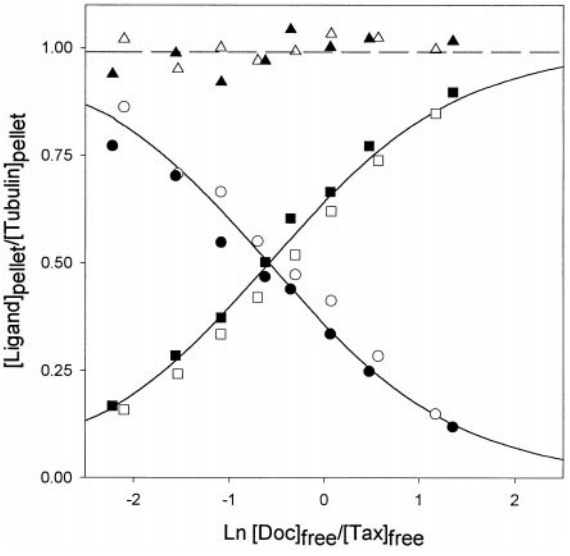

FIG. 2. **Equilibrium competition measurements of the exchange of bound Taxol and docetaxel in microtubules.** The binding of each taxoid to the microtubule pellet is plotted *versus* the natural logarithm the ratio of their free concentrations measured in the supernatant. GDP-tubulin (11.3 μM) was assembled at 37 °C in PEDTA buffer, 8 mM $MgCl_2$, by the addition of one of the taxoids at a concentration equal or larger than 11 μM. One hour after the other ligand was added to complete a total taxoids concentration of 25 μM, and samples were incubated for 1 additional hour. The concentration of assembled tubulin was 11.0 ± 0.2 μM and the concentration of unassembled tubulin in the supernatants varied between 0.25 μM in docetaxel excess and 0.42 μM in Taxol excess. *Filled circles*, Taxol bound per assembled tubulin dimer; *filled squares*, docetaxel bound; *filled triangles*, total taxoid bound. The respective *empty symbols* are the results of directly assembling the microtubules with the mixture of both Taxol and docetaxel from the begining of the experiment. The *solid lines* are the model binding curves calculated for the competition of Taxol and docetaxel for one site per assembled tubulin dimer, with a relative affinity docetaxel/Taxol of 1.8 (18). The *dashed line* is the average of the total taxoid binding in both experiments.

scattering maxima with time were fitted with the pertinent functions employing a least squares Marquardt algorithm (Sigmaplot, Jandel Scientific).

RESULTS

Taxoid Binding and Dissociation from Assembled Microtubules—Microtubules were first assembled to steady state from purified GTP-tubulin in glycerol-containing buffer, and excess

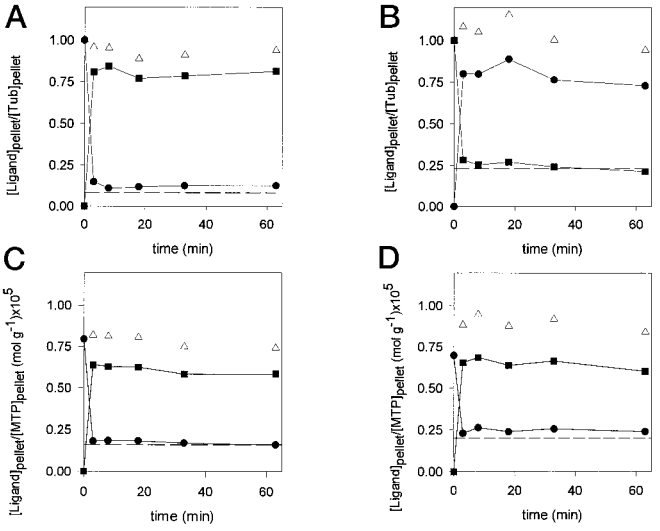

FIG. 3. **Time course of taxoid displacement in microtubules.** *A,* GDP-tubulin (9.5 μM in PEDTA buffer containing 1 mM GDP and 8 mM $MgCl_2$) was assembled with 10 μM Taxol during 1 h at 37 °C, the sample was diluted to 5 μM tubulin, 5.3 μM Taxol, 30 μM docetaxel was immediately added to the solution, and samples were taken at different times of reaction. *Circles*, Taxol binding; *squares,* docetaxel binding; *dashed line,* theoretical Taxol binding at equlibrium, with a 1.8 binding constant ratio (docetaxel/Taxol, see Fig. 2); *open triangles*, total ligand bound. *B,* tubulin was assembled with 10 μM docetaxel, the sample was diluted to 3 μM tubulin, 3.2 μM docetaxel, 20 μM Taxol was immediately added to the solution, and samples were taken at different times of reaction. *Symbols* are as in *panel A*, except that the *dashed line* is the theoretical docetaxel binding at equilibrium. The use of a larger excess of the displacing drugs which would have lead to larger displacements was precluded by their low solubility. To avoid any precipitation problems the concentration of free Taxol should be kept under 10 μM, and free docetaxel should be kept under 30 μM under these conditions. *C,* microtubule protein (0.88 mg ml^{-1} tubulin and MAPs) was assembled with 10 μM Taxol during 1 h at 37 °C, the sample was diluted to 0.5 mg ml^{-1} protein, 5.7 μM Taxol, 30 μm docetaxel was immediately added and samples collected at the time indicated. *D,* the microtubule protein was assembled with 10 μM docetaxel, diluted to 0.33 mg ml^{-1} to 3.7 μM docetaxel and 30 μM Taxol added. *Symbols* in *panels C* and *D* are as in *panel A* and the *dashed lines* are the theoretical ligands binding at equilibrium, assuming the same relative affinities as in microtubules made of purified tubulin.

Taxol or docetaxel were added to them. Since taxoid binding and assembly are coupled, an additional fraction of tubulin will assemble. However, choosing an initial concentration of tubulin 10–25-fold larger than the critical concentration for assembly reduces the newly assembled protein to a few percent of total, giving an acceptably small perturbation of the system (Fig. 1). Under these conditions, the binding of radioactively labeled taxoids to microtubules, measured 30 min after Taxol or docetaxel addition by sedimentation in a table top ultracentrifuge, was 0.98 ± 0.06 molecules of taxoid per tubulin heterodimer. An alternative interpretation would be that taxoids were not binding to preassembled microtubules, but that due to dynamic instability, most microtubules fully depolymerized and reassembled with bound taxoid during the experiment. However, since Taxol is known to suppress microtubule dynamics (21), we concluded that in these experiments taxoids were most probably directly binding to the assembled microtubules.

Next we turned to measuring taxoid exchange in microtubules assembled from GDP-tubulin, which are necessarily devoid of dynamic instability (since there is no GTP to be hydrolyzed). Microtubules were previously assembled with Taxol in equimolecular or larger ratios with tubulin, docetaxel was added to them keeping the total concentration of taxoids constant, and the binding of each taxoid was measured. The re-

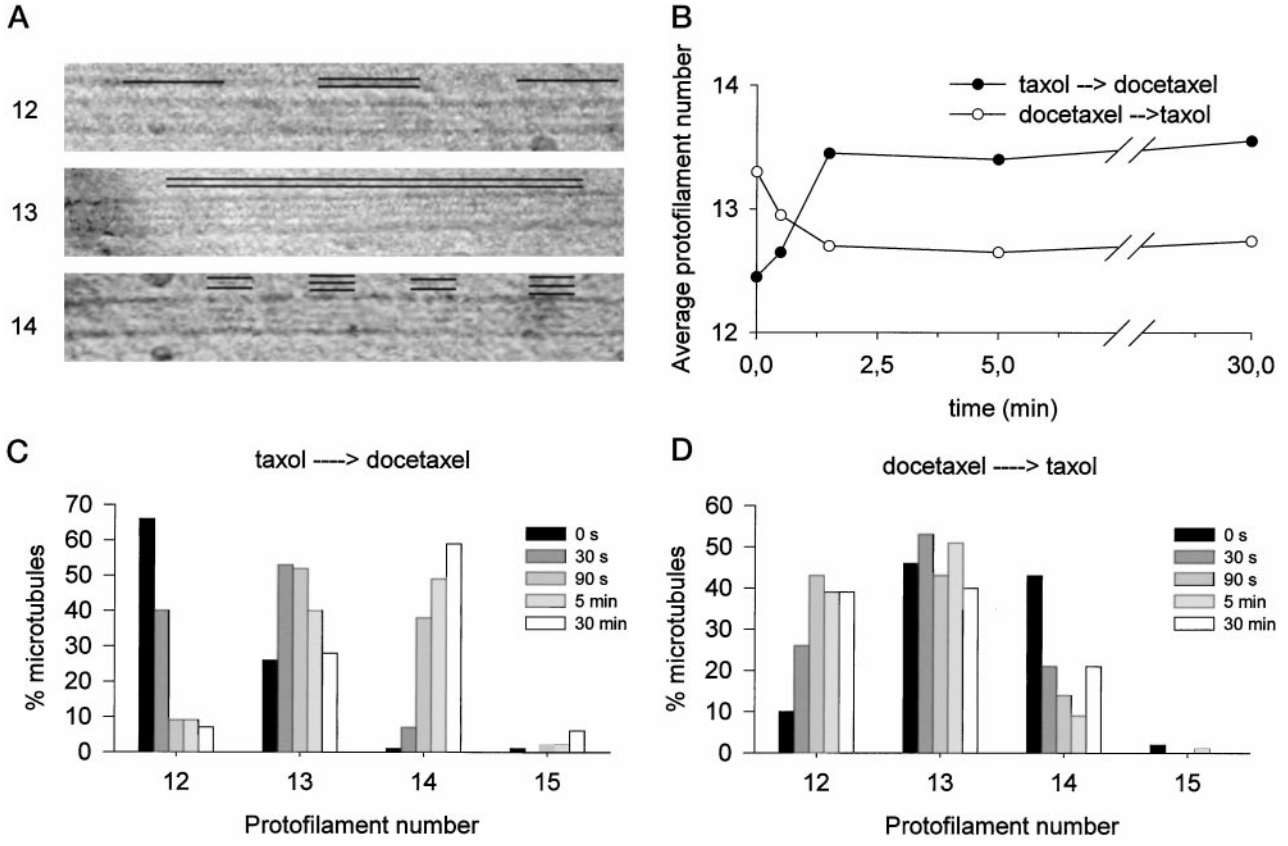

FIG. 4. **Changes in microtubule protofilament number induced by taxoid displacement, determined by cryoelectron microscopy.** Microtubules were assembled from 10 μM GDP-tubulin as described under "Experimental Procedures." *A,* examples of three different types of microtubule images employed to classify their number of protofilaments. Characteristic dark fringe patterns for 12 (2-1-2 fringes), 13 (2 nearly continuous fringes, slightly off-center), and 14 protofilaments (3-2-3 fringes) (27, 51) can be observed along the center of microtubules. These are indicated by the *lines* drawn on *top* of each microtubule. *B,* average protofilament number of the microtubules population upon taxoid exchange. *C,* distribution of the microtubules population according to their number of protofilaments after incubation at different times (0, 0.5, 1.5, and 30 min) of Taxol-induced microtubules with excess docetaxel. Approximately 100 microtubules were counted per sample. *D,* the same for docetaxel-induced microtubules with excess Taxol.

sults (Fig. 2, *solid symbols*) showed that at binding equilibrium Taxol had dissociated and docetaxel had bound to microtubules, competing for binding to one site per assembled tubulin dimer (docetaxel has a relative apparent affinity 1.8 times larger than that of Taxol, indicated by the model binding competition shown by the *solid lines* in Fig. 2). In control measurements both ligands were added before assembly (18), giving an equilibrium mixture of Taxol and docetaxel-liganded sites which was practically coincident with the experiment (Fig. 2, *empty symbols*; see Fig. 7 and equations for ligand competition in Ref. 18). The same results were obtained with GTP-tubulin (not shown).

The kinetics of taxoid exchange were examined by diluting microtubules assembled with Taxol into a 6-fold excess of docetaxel and vice versa. The results (Fig. 3, *A* and *B,* respectively) indicated that 95% or more of the maximal taxoid exchange had taken place in 3 min (the system had practically re-equilibrated by the dead time of the sedimentation method). Note that, in a rough approximation, this would imply a half-life of about 40 s or less for a hypothetical first order displacement reaction. The final number of molecules of each taxoid bound per microtubule-assembled tubulin dimer corresponded to its relative affinity and concentration. Control measurements of the pelleted protein showed that the taxoid microtubules did not depolymerize by dilution during the experiment. Similar results were obtained with GTP-tubulin (not shown). When these measurements were made with microtubules assembled from tubulin with microtubule-associated proteins, essentially the same result was obtained (except that the stoichiometry of taxoid binding was reduced to 0.7–0.8 mol of ligand per 100,000 g of protein; Fig. 3, *C* and *D*). This indicated that MAPs modified neither the accessibility of the microtubule Taxol-binding site, within the limited time resolution of the experiment, nor the relative affinities of docetaxel and Taxol.

Electron Microscopy of Microtubules during Taxoid Exchange—Electron micrographs of negatively stained samples of microtubules from the taxoid-binding and displacement experiments described above indicated significant changes in the protofilament distribution of the microtubule population, determined by counting their characteristic fringe patterns ("Experimental Procedures" and Fig. 4*A*). These consisted in a transition from the glycerol distribution (average 13.1 protofilaments in these negative stained samples) to the Taxol distribution (average 12.3 protofilaments) upon Taxol addition, whereas addition of docetaxel did not modify the distribution of protofilament numbers (average 13.2). On the other hand, addition of excess docetaxel to Taxol microtubules changed the distribution to the docetaxel one, and addition of Taxol to docetaxel microtubules reduced the number of protofilaments to the Taxol values (not shown). Surprisingly, these changes had practically taken place 1 min after taxoid addition.

Since negatively stained dehydrated microtubules are frequently flattened onto the grid, in order to avoid possible artifacts and to reach a shorter preparation time, we repeated the taxoid exchange experiments using cryoelectron microscopy of vitrified specimens. Fig. 4 shows distributions of protofilament numbers of microtubules assembled from GDP-tubulin and taxoid. Different samples were instantaneously frozen at 0, 0.5,

1.5, 5, and 30 min after addition of the competing taxoid in displacement experiments. The average protofilament number (Fig. 4*B*) and the distributions in each sample (Fig. 4, *C* and *D*) indicated that upon exchange of the bound taxoid in the population of assembled microtubules the protofilament number had relaxed toward that characteristic of each taxoid (averages of 12.4 and 13.3 protofilaments for Taxol and docetaxel, respectively). The half-time of this change was roughly the same as the shortest time of sample preparation, *i.e.* 0.5 min (Fig. 4*B*).

X-ray Scattering Changes Induced by Taxoid Binding to Microtubules—Solutions of glycerol-, Taxol-, and docetaxel-induced microtubules give characteristic differences in their x-ray scattering profiles. These consist of (i) an inward displacement in Taxol microtubules of the maxima of the J_0 Bessel function (corresponding to the low resolution transform of the excess electron density of the microtubule hollow cylinders), which serves to measure the different mean diameter (protofilament number) of each microtubule population and (ii) a small inward displacement of the J_n and J_{n-3} Bessel function maxima in both types of taxoid induced microtubules with respect to glycerol microtubules (27, 28). The latter is compatible with an increase in the spacing between tubulin monomers along the microtubule protofilament (38, 39).

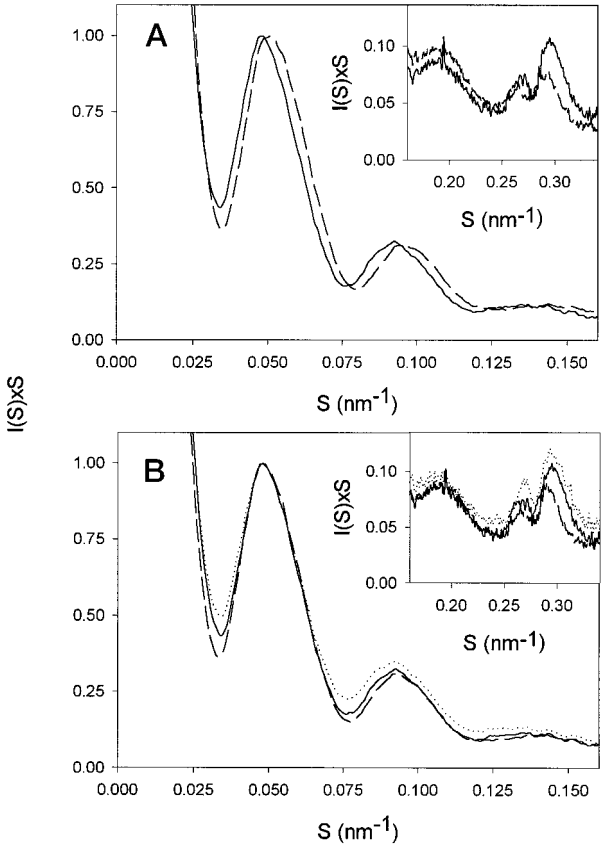

FIG. 5. **Taxoid-induced changes in microtubule x-ray scattering.** The corrected intensity profiles of microtubules assembled from 130 μM GTP-tubulin in glycerol assembly buffer at 37 °C are shown. *A,* 1 h after assembly 1% Me_2SO (*solid line*) or 150 μM Taxol, 1% Me_2SO (*dashed line*) were manuallly mixed into the solution. *B,* 1 h after assembly 150 μM docetaxel, 1% Me_2SO (*dashed line*), or 100 μM colchicine, 1% Me_2SO (*dotted line*) were added (the *solid line* is the same as in *panel A*, shown for comparison). Measurements were accumulated for 15 min, starting 5 min after the additions. The *insets* show enlargements of the area from 0.15 to 0.35 nm^{-1}.

Microtubules were assembled to steady state in glycerol-containing buffer, Taxol, docetaxel, or solvent were added to them and their x-ray scattering profiles were acquired during the following 5–20 min (Fig. 5). Measurements of the position of each maxima (Table I) show that (i) from the displacement of the J_0 maxima upon Taxol binding, the mean diameter of the glycerol microtubule population (24.3 nm) decreases to a value (22.5 nm) characteristic of Taxol-induced microtubules (22 nm), while the binding of docetaxel does not significantly modify it and (ii) both taxoids induce the same small shift in the position of the J_3 and J_{n-3} maxima. Addition of the microtubule assembly inhibitor colchicine modified insignificantly the scattering pattern of glycerol-induced microtubules in the time scale of the experiment (Fig. 5*B*). It could be argued that during the time of the measurement each glycerol microtubule may totally depolymerize and new microtubules reassemble with bound Taxol. However, a second series of ligand exchange experiments were performed in which microtubules were assembled with glycerol plus Taxol to suppress dynamic instability (21), and an excess of docetaxel added, or vice versa. The results (Table II) showed displacement of the J_0 maxima near the values of docetaxel and Taxol microtubules.

Finally, the time course of the change in position of the J_{01} and J_{02} maxima induced by Taxol on glycerol microtubules was monitored employing a fast mixing device built for this type of x-ray scattering experiments (56). The results showed a time-dependent displacement between the expected values, distinct from the noise of the individual kinetic measurement, and with a half-time of approximately 60 s (Fig. 6) under the conditions of these experiments.

DISCUSSION

How Can in Vitro Assembled Microtubules Exchange Protofilaments?—Since the binding of taxoids during tubulin assembly is known to modulate the protofilament number of microtubules (Introduction), one important question to answer was whether the structure of preformed microtubules would change upon binding of Taxol. The electron microscopy results indicate that the number of protofilaments of microtubules made of

TABLE I

Ligand-induced changes in the position of the x-ray solution scattering maxima of microtubules previously assembled from GTP-tubulin in glycerol buffer

Tubulin (at concentrations ranging from 120 to 190 μM) was assembled in glycerol assembly buffer for 30 min at 37 °C. An equimolecular concentration of taxoid, colchicine, or their solvent (1.5% dimethyl sulfoxide) were added. The x-ray scattering profiles were acquired for the next 5–20 min. Deviations in the measurements of the position of the J_0 and the $J_{n,3,n-a}$ maxima wre typically ±0.002 and ±0.001 nm^{-1}, respectively.

Ligand added	Scattering maxima and position						Mean helical radius
	J_{01}	J_{02}	J_{03}	J_n	J_3	J_{n-3}	
			nm^{-1}				*nm*
None	0.050	0.092	0.139	0.192	0.264	0.289	12.1
Taxol	0.053	0.099	0.147	0.192	0.256	0.284	11.3
Docetaxel	0.050	0.093	0.140	0.193	0.256	0.283	12.0
Colchicine	0.050	0.090	0.137	0.192	0.265	0.289	12.2
Taxol before assembly[a]	0.055	0.103	0.154	0.193	0.256	0.285	10.8
Docetaxel before assy[a]	0.050	0.092	0.137	0.193	0.256	0.285	12.1

[a] Reference values of microtubules assembled with each taxoid (28).

TABLE II
Changes in microtubule thickness induced by taxoid exchange, measured with x-ray scattering

GTP-tubulin (76 μM) was assembled with equimolecular taxoid for 30 min at 37 °C in glycerol assembly buffer. The other taxoid (100 μM) was then added and x-ray scattering measured within 5–20 min.

Ligand added before assembly	Ligand added after assembly	J_{01}	J_{02}	Mean helical radius
		nm^{-1}		nm
None	None	0.050	0.091	12.2
Taxol	Docetaxel	0.051	0.095	11.7
Docetaxel	Taxol	0.052	0.099	11.2
Taxol	None	0.053	0.102	10.9
Docetaxel	None	0.050	0.092	12.1
None	Taxol	0.053	0.099	11.2
None	Docetaxel	0.050	0.092	12.1

purified GDP-tubulin (devoid of dynamic instability) changes in seconds upon taxoid substitution (docetaxel for Taxol or vice versa). The static x-ray scattering results provide independent quantitative confirmation with microtubules preassembled from GTP-tubulin and with empty Taxol sites, even at longer measuring times and larger protein concentrations. In addition, they confirm a taxoid-induced change in the spacings of the microtubule lattice. The possibility that the latter microtubules had disassembled due to dynamic instability and reassembled with Taxol seems unlikely, due to Taxol suppression dynamic instability. Moreover, pushing time-resolved x-ray scattering measurements of microtubules to the limit and using a fast mixing device (Fig. 6) has permitted monitoring the change in microtubule diameter upon Taxol addition, which took place with a half-time in the order of 1 min.

In order to explain these results, we hypothesize that taxoid-bound microtubules have considerable internal dynamics enabling the addition and loss of protofilaments in a relatively short time scale, even their end-dynamic instability is frozen. Binding of the taxoid may induce the dynamic opening of the microtubule wall, or alternately, this may be an intrinsic property of glycerol-induced microtubules without taxoid, permitting Taxol binding and the resulting change in protofilament composition. The process might be envisaged as moving microdefects in the microtubule lattice or as constant opening and closing of seams along the microtubule wall, by means of reversible dissociation of the relatively weak lateral interactions between protofilaments. Having a given percent of opened microtubules at a steady state of assembly is not incompatible with the x-ray scattering profiles of microtubules (see Fig. 2 in Ref. 28). This transient opening may or may not correspond to the structural seam of the microtubule lattices, to frequent electron microscopy observations of opening microtubule walls, and to microtubule opening with large taxoid excess (28). In fact, non-taxoid microtubules grow at their ends in the form of sheets which then close (4), during taxoid-induced assembly large open microtubular sheets form which later close into microtubules (29), and what we are now proposing could be a kind of reverse process. Our observations of taxoid-induced change in protofilament number pertain to microtubules made of purified tubulin. MAPs permit taxoid binding to and dissociation from microtubules (see "Results"), yet microtubules assembled with MAPs and Taxol have an unmodified protofilament number (27). Similarly, the change in axial spacing between tubulin monomers in microtubules assembled with Taxol (39) has not been observed when microtubules are decorated with kinesin (57). Nevertheless, in studies with microtubule motor proteins (see Introduction) the possibility of transient opening of Taxol microtubules should be considered.

How Does Taxol Reach Its Binding Site in Microtubules?—

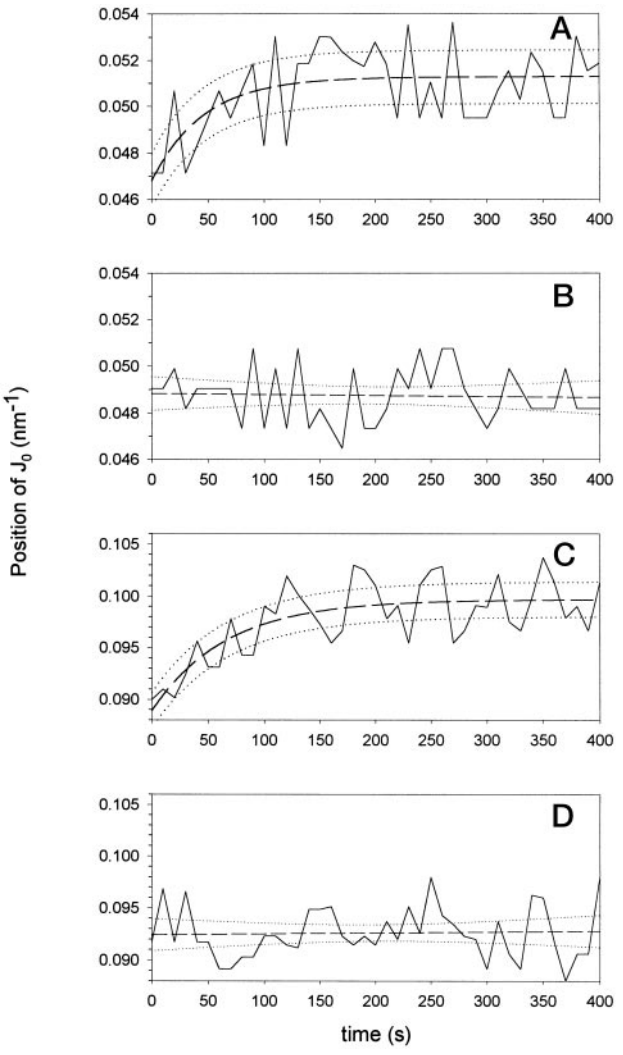

FIG. 6. **Time course of the Taxol-induced change in position of the J_0 x-ray scattering maxima of microtubules.** *A,* a solution of assembled microtubules (67 μM GTP-tubulin in glycerol assembly buffer containing 7 mM $MgCl_2$, 37 °C), was supplemented at time 0 with Taxol (70 μM, 2.5% residual Me_2SO), employing an isothermal fast mixing device ("Experimental Procedures"). The position of the J_{01} maximum is plotted every 10 s. *B,* a control of experimental noise made by mixing Me_2SO into microtubules (50 μM tubulin, 50 μM docetaxel) in the same buffer. *C* and *D* are plots of the position of the J_{02} maximum in the same experiments as *A* and *B,* respectively. The *dashed lines* represent the best exponential or linear fits to the data and the *dotted lines* the 95% confidence interval of each fit. The average positions and 95% confidence intervals in the plateau regions in *A-D* are, respectively, 0.0510 ± 0.0007, 0.0487 ± 0.0003, 0.0996 ± 0.0013, and 0.0926 ± 0.007 nm^{-1}, also showing a significant movement of the scattering maxima in *A* and *C*.

The taxoid-binding site has been found readily accessible in assembled microtubules. This holds for microtubules assembled with empty taxoid-binding sites as well as for taxoid exchange in taxoid-induced microtubules, made of purified tubulin or tubulin plus MAPs. This is supported by the rapid Taxol-induced increase of flexibility of assembled microtubules (40). Moreover, fluorescent taxoids (58) specifically and efficiently label *in vitro* assembled and cellular microtubules by binding near a microtubule surface (48). These characteristics would be compatible with binding of taxoids in a zone between protofilaments (27–29, 59), near the outer microtubule surface. However, in the high resolution structure of tubulin in Taxol-stabilized zinc sheets, Taxol is at one side of the β-tubulin monomer, clearly in the protein face assigned to the microtu-

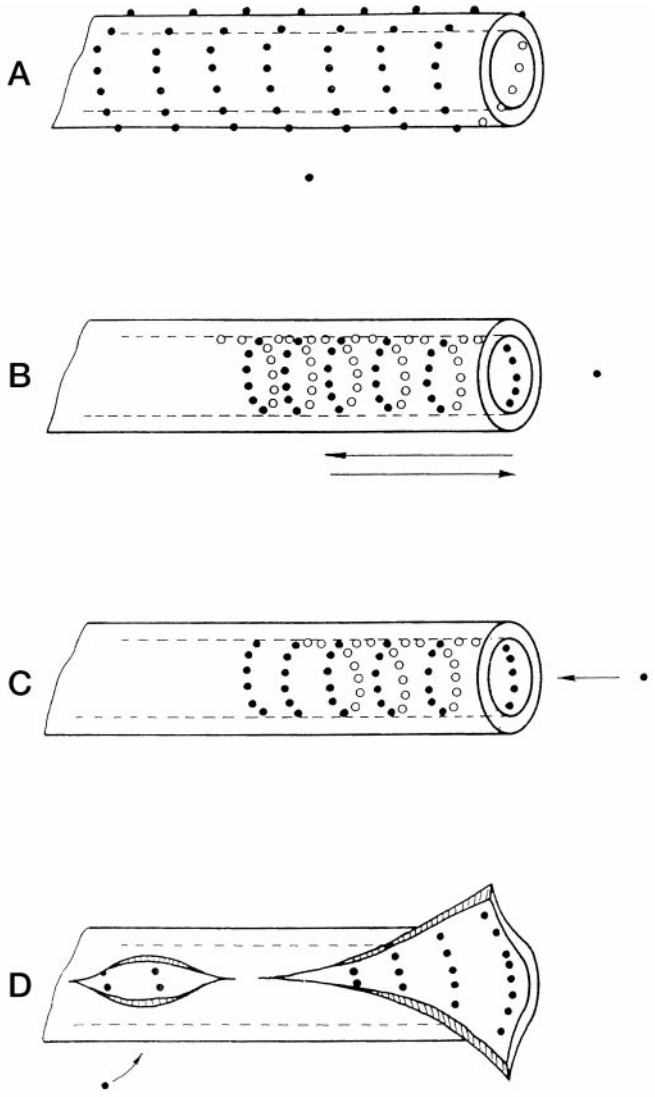

FIG. 7. **Schematic representation of different hypotheses on how Taxol may reach its binding site at the outer (*A*) or the inner (*B–D*) microtubule surface (see "Discussion").** *A,* Taxol binds at the outer microtubule surface. *B,* Taxol binds at the inner microtubule surface and its access from the solution into the lumen is facilitated by microtubule dynamic instability. *Closed* and *open circles* represent Taxol molecules in the front and back of the lumen, respectively. *C,* Taxol diffuses from the bulk solution through the microtubule ends and binds into the microtubule lumen. *D,* entry of Taxol into the microtubule lumen through openings between protofilaments in the microtubule wall. This might be envisaged as relatively large pores, or as dynamic lattice microdefects (the size is exaggerated in the scheme) or as opening and closing of seams between protofilaments from the microtubule ends.

bule lumen (49, 60).[2] In principle, the types of hypotheses which may be considered include (Fig. 7) those discussed below.

Taxol Binds Near the Outer Microtubule Surface (Fig. 7A)—The location of Taxol in zinc sheets (49) would not be applicable to microtubules, although it makes sense with photoaffinity labeling results (7, 8). In fact, this is the simplest interpretation of our data on the accessibility of the taxoid-binding site.

On the other hand, having the Taxol-binding site at the microtubule lumen is not necessarily incompatible with our results, if one chooses the inner microtubule surface. The apparently more difficult problem is to understand how do taxoids (this study) and fluoresceinated Taxol (48) get there when they bind to preassembled microtubules. This leads to the next possibilities.

Taxol Binds into the Lumen Due to Microtubule Dynamic Instability, Permitting Endwise Depolymerization and Reassembly with Taxoid (Fig. 7B)—However, the taxoid exchange experiments with microtubules assembled from GDP-tubulin practically rule out this possibility. In addition, the labeling of microtubules with fluorescent taxoid in permeabilized cells takes place in less than 1 min (see Fig. 8 in Ref. 48), which is faster than typical microtubule turnover times. This does not preclude taxoid binding by microtubule dynamic instability in treated living cells, at zones of active microtubule growth (see Fig. 9 in Ref. 48).

Taxol Diffuses Through the Open Microtubule Ends and Binds into the Lumen (Fig. 7C)—Small solute diffusion into microtubules may be fast enough (in the sub-second time scale), however, the process taking place is diffusion-limited binding to a large effective concentration of binding sites in the microtubule lumen (48, 61). This mechanism should be length-dependent. The time required for Taxol to fill a distance, x, inside microtubules can be estimated as $t = ([B]_0/[A])\, x^2/2D$, where $[A]$ is the free ligand concentration in the bulk solution, $[B]_0$ the equivalent total concentration of binding sites inside microtubules (the concentration of tubulin dimers per microtubule inner volume, which is ~0.01 M), and D the diffusion coefficient of the small ligand (~$2\ 10^{-6}$ $cm^2\ s^{-1}$) (48). The minimal binding time calculated under the present conditions (20 μM Taxol and a 5-μm microtubule length) is ~0.5 min. This is within the dead time of the taxoid exchange measurements and the 0.5–1 min of the resulting microtubule structural change ("Results"). However, the rapid binding of fluorescent taxoid to microtubules was previously considered to argue against this possibility (48). In addition, preliminary results obtained by monitoring the large change in emission anisotropy of fluoresceinated Taxol upon binding (48) indicate that the association of 20 μM fluorescent taxoid to microtubule-assembled tubulin (20 μM) has surprisingly taken place in 2 s, both with native and fragmented microtubules.

Taxol Diffuses through the Microtubule Wall and Binds into the Lumen (Fig. 7D)—It is difficult to know whether pores in present low resolution models of microtubules (13, 14, 30, 53, 62)) are really large enough for the size of Taxol and fluorescent taxoids, their flexibility, and partial hydrophobic character (48, 63) (note that having pores larger than the ligand becomes chemically indistinguishable from mechanism A, and that mechanisms A and D should essentially be independent of microtubule length). Alternately, moving lattice defects might permit ligand diffusion through the microtubule wall, or a large opening or breathing of the microtubule structure might occur.

Therefore, excluding dynamic instability (mechanism B), the available kinetic data favors mechanisms A or D more than C. A crucial issue is to obtain an independent confirmation of the locus of taxoid binding at the inner or outer microtubule surface in *in vitro* assembled and cellular microtubules.

Taxol at the Microtubule Lumen: A New Cytoplasmic Compartment?—The above discussed binding results together with the locus of Taxol binding at the microtubule lumen, deduced from the 3.7-Å model structure of tubulin in Taxol-stabilized

[2] Note that structural contradictions have been frequent in the microtubule field, including microtubule polarity and the mode of binding of microtubule motors (discussed in Ref. 66). In the present case, not having the Taxol-binding site at the microtubule lumen would imply a gross error in the location of the site (based on structural and affinity labeling results) or in the translation of the dimer from zinc sheets into microtubules (which is constrained by placing the tubulin C termini at the microtubule surface). It is difficult to explain how this could happen. Such circumstances would not affect the results and main conclusions of the present study, but only the suggestion of in the last section of the "Discussion."

zinc sheets (49), may be interpreted to suggest a porous structure or breathing of the walls of microtubules *in vitro* and in permeabilized cells, in order to allow access of taxoids to the inner microtubule surface. The *in vitro* observed protofilament number change, however, would not apply to cells, where the protofilament number is stabilized by microtubule nucleating centers and by proteins binding to the outer microtubule surface. Having the Taxol-binding site inside microtubules would render the inner microtubule surface potentially functional in unexpected interactions with relatively small cellular molecules (48), irrespective of the mechanism by which Taxol might enter the microtubule lumen, through the ends or across the microtubule wall. Note that in the model structure of the tubulin dimer (49), the post-translationally acetylable α-tubulin Lys-40 residue (a modification believed to take place in assembled stable microtubules; reviewed in Ref. 64) within one of the more variable zones among tubulin sequences, is in a large loop which is also facing the microtubule lumen.[2] It was suggested that Taxol is a possible surrogate of endogenous microtubule ligands (10, 65). Whereas motor proteins and MAPs bind to the outer surface of microtubules, interacting with the C-terminal domain of tubulin, small ligands could bind to their inner surface. Actually, the size of the microtubule lumen (about 15 nm diameter) is enough to permit access of even large globular proteins, which will encounter a large effective concentration of confined potential binding sites, the inner faces of the tubulin molecules. This potential functional role has previously been overlooked. It is therefore possible that the microtubule lumen may constitute an active, newly discovered cytoplasmic compartment, instead a simple solvent-filled cavity resulting from microtubule architecture.

Acknowledgments—We especially thank Dr. J. L. Carrascosa (Centro Nacional de Biotecnologia, CSIC, Madrid) for making cryoelectron microscopy available and careful suggestions to the manuscript, and Dr. Y. Engelborghs (Katholieke Universiteit Leuven) for providing the fast mixing device for the x-ray scattering measurements and encouragement. We thank Dr. M. Kikkawa for calling our attention to microtubule pores, Drs. A. P. Minton, A. U. Acuña, and P. Lillo for discussions, A. Gleeson, Drs. D. Leynadier, and C. Dumortier for help during x-ray measurements, Drs. I. Ringel and S. B. Horwitz for [^{3}H]Taxol, and Rhone-Poulenc Rorer for docetaxel and [^{14}C]docetaxel.

REFERENCES

1. Menéndez, M., Rivas, G., Díaz, J. F., and Andreu, J. M. (1998) *J. Biol. Chem.* **273,** 167–176
2. Kirchner, K., and Mandelkow, E. M. (1985) *EMBO J.* **4,** 2397–2402
3. Downing, K. H., and Nogales, E. (1998) *Curr. Opin. Cell Biol.* **10,** 16–22
4. Chrétien, D., Fuller, S. D., and Karsenti, E. (1995) *J. Cell Biol.* **129,** 1311–1328
5. Heald, R., Tournebize, R., Blank, T., Sandaltzopoulos, R., Becker, P., Hyman, A., and Karsenti, E. (1996) *Nature* **382,** 420–425
6. Horwitz, S. B. (1992) *Trends Pharmacol. Sci.* **13,** 134–136
7. Rao, S., Krauss, N. E., Heerding, J. M., Swindell, C. S., Ringel, I., Orr, G. A., and Horwitz, S. B. (1994) *J. Biol. Chem.* **269,** 3132–3134
8. Rao, S., Orr, G. A., Chaudhary, A. G., Kingston, D. G. I., and Horwitz, S. B. (1995) *J. Biol. Chem.* **270,** 20235–20238
9. Jordan, M. A., and Wilson, L. (1998) *Curr. Opin. Cell Biol.* **10,** 123–130
10. Schiff, P. B., Fant, J., and Horwitz, S. B. (1979) *Nature* **277,** 665–667
11. Kocielski, F., Arnal, I., and Wade, R. H. (1998) *Curr. Biol.* **8,** 191–198
12. Thormälen, M., Marx, A., Müller, S. A., Song, Y. H., Mandelkow, E. M., Aebi, U., and Mandelkow, E. (1998) *J. Mol. Biol.* **275,** 795–809
13. Hoenger, A., Sack, S., Thormählen, M., Marx, A., Müller, J., Gross, H., and Mandelkow, E. (1998) *J. Cell Biol.* **141,** 419–430
14. Hirose, K., Cross, R. A., and Amos, L. A. (1998) *J. Mol. Biol.* **278,** 389–400
15. Hancock, W. O., and Howard, J. (1998) *J. Cell Biol.* **140,** 1395–1405
16. Romberg, L., Pierce, D. W., and Vale, R. D. (1998) *J. Cell Biol.* **140,** 1407–1416
17. Chau, M. F., Radeke, M. J., Barasoain, I., de Inés, C., Kohlstaedt, L. A., and Feinstein, S. C. (1998) *Biochemistry*, in press
18. Díaz, J. F., and Andreu, J. M. (1993) *Biochemistry* **32,** 2747–2755
19. Díaz, J. F., Menendez, M., and Andreu, J. M. (1993) *Biochemistry* **32,** 10067–10077
20. Caplow, M., Shanks, J., and Ruhlen, R. (1994) *J. Biol. Chem.* **269,** 23399–23402
21. Derry, W. B., Wilson, L., and Jordan, M. A. (1995) *Biochemistry* **34,** 2203–2211
22. Tilney, L. G., Brian, J., Bush, D. J., Fujiwara, K., Mooseker, M. S., Murphy, D. B., and Snyder, D. H. (1973) *J. Cell Biol.* **59,** 267–275
23. Chrétien, D., Metoz, F., Verde, F., Karsenti, E., and Wade, R. H. (1992) *J. Cell Biol.* **117,** 1031–1040
24. Lanzavecchia, S., Bellon, P. L., Dallai, R., and Afzelius, B. A. (1994) *J. Struct. Biol.* **113,** 225–237
25. Hirose, K., Lockhart, A., Cross, R. A., and Amos, L. A. (1996) *Proc. Natl. Acad. Sci. U. S. A.* **93,** 9539–9544
26. Raff, E. C., Fackenthal, J. D., Hutchens, J. A., Hoyle, H. D., and Turner, F. R. (1997) *Science* **275,** 70–73
27. Andreu, J. M., Bordas, J., Díaz, J. F., García de Ancos, J., Gil, R., Medrano, F. J., Nogales, E., Pantos, E., and Towns-Andrews, E. (1992) *J. Mol. Biol.* **226,** 169–184
28. Andreu, J. M., Díaz, J. F., Gil, R., de Pereda, J. M., García de Lacoba, M., Peyrot, V., Briand, C., Towns-Andrews, E., and Bordas, J. (1994) *J. Biol. Chem.* **269,** 31785–31792
29. Díaz, J. F., Andreu, J. M., Diakun, G., Towns-Andrews, E., and Bordas, J. (1996) *Biophys. J.* **70,** 2408–2420
30. Beese, L., Stubbs, G., and Cohen, C. (1987) *J. Mol. Biol.* **194,** 257–264
31. Hyman, A. A., Chretien, D., Arnal, I., and Wade, R. H. (1995) *J. Cell Biol.* **128,** 117–125
32. Howard, W. D., and Timasheff, S. N. (1986) *Biochemistry* **25,** 8292–8300
33. Melki, R., Carlier, M. F., Pantaloni, D., and Timasheff, S. N. (1989) *Biochemistry* **28,** 9143–9152
34. Mandelkow, E. M., Mandelkow, E., and Milligan, R. A. (1991) *J. Cell Biol.* **114,** 977–991
35. Díaz, J. F., Pantos, E., Bordas, J., and Andreu, J. M. (1994) *J. Mol. Biol.* **238,** 214–223
36. Hyman, A. A., and Karsenti, E. (1996) *Cell* **84,** 401–410
37. Müller-Reichert, T., Chrétien, D., Severin, F., and Hyman, A. A. (1998) *Proc. Natl. Acad. Sci. U. S. A.* **95,** 3661–3666
38. Vale, R. D., Coppin, C. M., Malik, F., Kull, F. J., and Milligan, R. A. (1994) *J. Biol. Chem.* **269,** 23769–23775
39. Arnal, I., and Wade, R. H. (1995) *Curr. Biol.* **5,** 900–908
40. Dye, R. B., Fink, S. P., and Williams, R. C., Jr. (1993) *J. Biol. Chem.* **268,** 6847–6850
41. Venier, P., Maggs, A. C., Carlier, M. F., and Pantaloni, D. (1994) *J. Biol. Chem.* **269,** 13353–13360
42. Mickey, B., and Howard, J. (1995) *J. Cell Biol.* **130,** 909–917
43. Kurz, J. C., and Williams, R. C. (1995) *Biochemistry* **34,** 13374–13380
44. Felgner, H. O., Müller, O., and Schliwa, M. (1996) *J. Cell Sci.* **109,** 509–516
45. Felgner, H. O., Frank, R., Biernat, J., Mandelkow, E. M., Mandelkow, E., Ludin, B., Matus, A., and Schliwa, M. (1997) *J. Cell Biol.* **138,** 1067–1075
46. Bras, W., Diakun, G. P., Díaz, J. F., Maret, G., Kramer, H., Bordas, J., and Medrano, F. J. (1998) *Biophys. J.* **74,** 1509–1521
47. Parness, J., and Horwitz, S. B. (1981) *J. Cell Biol.* **91,** 479–487
48. Evangelio, J. A., Abal, M., Barasoain, I., Souto, A. A., Lillo, M. P., Acuña, A. U., Amat-Guerri, F., and Andreu, J. M. (1998) *Cell Motil. Cytoskeleton* **39,** 73–90
49. Nogales, E., Wolf, S. G., and Downing, K. (1998) *Nature* **391,** 199–203
50. De Pereda, J. M., Wallin, M., Billger, M., and Andreu, J. M. (1995) *Cell Motil. Cytosketon* **30,** 153–163
51. Chrétien, D., and Wade, R. H. (1991) *Biol. Cell* **71,** 161–174
52. Ray, S., Meyhofer, E., Milligan, R. A., and Howard, J. (1993) *J. Cell Biol.* **121,** 1083–1093
53. Sosa, H., and Milligan, R. A. (1996) *J. Mol. Biol.* **260,** 743–755
54. Chrétien, D., Kenney, J. M., Fuller, S. D., and Wade, R. H. (1996) *Structure* **4,** 1031–1040
55. Andreu, J. M., García de Ancos, J., Starling, D., Hodgkinson, J. L., and Bordas, J. (1989) *Biochemistry* **28,** 4036–4040
56. Díaz, J. F., Strobbe, R., Engelborghs, Y., Chacón, P., Andreu, J. M., and Diakun, G. (1998) *Rev. Sci. Instrum.* **69,** 286–289
57. Marx, A., Thormälen, M., Müller, J., Sack, S., Mandelkow, E. M., and Mandelkow, E. (1998) *Eur. Biophys. J.* **27,** 455–465
58. Souto, A. A., Acuña, A. U., Andreu, J. M., Barasoain, I., Abal, M., and Amat-Guerri, F. (1995) *Angew. Chem. Intl. Ed. Engl.* **34,** 2710–2712
59. Nogales, E., Wolf, S. G., Khan, I. A., Ludueña, R. F., and Downing, K. H. (1995) *Nature* **375,** 424–427
60. Nogales, E., Downing, K. H., Amos, L. A., and Löwe, J. (1998) *Nature Struct. Biol.* **5,** 451–458
61. Odde, D. (1998) *Eur. Biophys. J.* **27,** 514–520
62. Kikkawa, M., Ishikawa, T., Wakabayashi, T., and Hirokawa, N. (1995) *Nature* **376,** 274–277
63. Jimenez-Barbero, J., Souto, A. A., Abal, M., Barasoain, I., Evangelio, J. A., Acuña, A. U., Andreu, J. M. and Amat-Guerri, F. (1998) *Bioorg. Med. Chem.,* in press
64. Ludueña, R. F. (1998) *Int. Rev. Cytol.* **178,** 207–275
65. Suffness, M. (1994) *In Vivo* **8,** 867–878
66. Egelman, E. H. (1998) *Curr. Biol.* **8,** R228–R290

Changes in Microtubule Protofilament Number Induced by Taxol Binding to an Easily Accessible Site: INTERNAL MICROTUBULE DYNAMICS

J. Fernando Di?az, José M. Valpuesta, Pablo Chacón, Greg Diakun and José M. Andreu

J. Biol. Chem. 1998, 273:33803-33810.
doi: 10.1074/jbc.273.50.33803